A *Caenorhabditis elegans* model of insulin resistance: Altered macronutrient storage and dauer formation in an OGT-1 knockout

John A. Hanover*†, Michele E. Forsythe*, Patrick T. Hennessey*, Thomas M. Brodigan‡, Dona C. Love*, Gilbert Ashwell*, and Michael Krause‡

Laboratories of *Cell Biochemistry and Biology and ‡Molecular Biology, National Institute of Diabetes and Digestive and Kidney Diseases, National Institutes of Health, Bethesda, MD 20892

Edited by Jeffrey M. Friedman, The Rockefeller University, New York, NY, and approved June 21, 2005 (received for review November 29, 2004)

O-linked *N*-acetylglucosamine (O-GlcNAc) is an evolutionarily conserved modification of nuclear pore proteins, signaling kinases, and transcription factors. The O-GlcNAc transferase (OGT) catalyzing O-GlcNAc addition is essential in mammals and mediates the last step in a nutrient-sensing "hexosamine-signaling pathway." This pathway may be deregulated in diabetes and neurodegenerative disease. To examine the function of O-GlcNAc in a genetically amenable organism, we describe a putative null allele of OGT in *Caenorhabditis elegans* that is viable and fertile. We demonstrate that, whereas nuclear pore proteins of the homozygous deletion strain are devoid of O-GlcNAc, nuclear transport of transcription factors appears normal. However, the OGT mutant exhibits striking metabolic changes manifested in a ≈3-fold elevation in trehalose levels and glycogen stores with a concomitant ≈3-fold decrease in triglycerides levels. In nematodes, a highly conserved insulin-like signaling cascade regulates macronutrient storage, longevity, and dauer formation. The OGT knockout suppresses dauer larvae formation induced by a temperature-sensitive allele of the insulin-like receptor gene *daf-2*. Our findings demonstrate that OGT modulates macronutrient storage and dauer formation in *C. elegans*, providing a unique genetic model for examining the role of O-GlcNAc in cellular signaling and insulin resistance.

nutrients | O-GlcNAc | signaling | diabetes mellitus

O-linked *N*-acetylglucosamine (O-GlcNAc) is a nucleocytoplasmic modification present throughout eukaryotic evolution with the possible exception of yeast (1, 2). Although many intracellular proteins such as nuclear pore components and transcription factors bear O-GlcNAc, the precise function of the modification is unknown. Evidence in mammals suggests a role for O-GlcNAc in the development of insulin resistance associated with noninsulin-dependent diabetes mellitus (3, 4). A number of lines of evidence also link O-GlcNAc to transcriptional regulation and neurodegeneration (1, 2). O-GlcNAc addition is partly driven by the levels of UDP-GlcNAc derived from the hexosamine biosynthetic pathway. This pathway is a nutrient-sensing pathway implicated in cellular signaling (1, 2). The uncertainty regarding the precise function of O-GlcNAc is perhaps to be expected given the many substrates modified by this glycan addition. Furthermore, O-GlcNAc is a dynamic modification; the levels of O-GlcNAc are maintained by the action of a glycosytransferase [O-linked GlcNAc transferase (OGT)] and a hexosaminidase (O-GlcNAcase) (1, 2). Mammalian O-GlcNAcase exists as two splice variants and is relatively specific for nucleocytoplasmic O-GlcNAc (1, 5, 6). The transferase, OGT, catalyzes the transfer of O-GlcNAc to Ser/Thr residues. This enzyme has been identified from a number of sources, including plants, human, rat, mouse, and the nematode *Caenorhabditis elegans* (7, 8). In plants, the OGT homolog *Spindly* is involved in plant-signaling pathways (9, 10). These evolutionarily conserved proteins share a similar overall structure; OGT is composed of multiple protein domains, including tetratricopeptide repeats and a catalytic domain composed of Rossman-like folds. We have recently solved the structure of the tetratricopeptide repeats of OGT and found that the repeats interact with target proteins via an Asn ladder similar to those found in importin α (11). The catalytic domain of OGT has also been suggested to have similarities to the glycogen phosphorylase superfamily (12).

In mammals, the gene encoding OGT is essential for embryonic and stem cell development and produces multiple transcripts resulting from alternative promoter usage and splicing (13–15). These OGT isoforms are differentially targeted to the nucleus and mitochondrion (15, 16). The presence of multiple isoforms and the embryonic lethality observed with mammalian knockouts has made analysis of the signaling functions of mammalian OGT difficult. Using a more targeted approach, OGT deletion has been linked to T cell apoptosis, neuronal τ hyperphosphorylation, and fibroblast growth arrest with altered expression of c-Fos, c-Jun, c-Myc, Sp1, and p27 (15). These studies strongly indicate that mammalian cells require a functional OGT allele.

To circumvent some of the problems encountered in examining mammalian OGT, we have chosen to examine the role of OGT in *C. elegans*. Previously, we identified a single gene (*K04G7.3*) encoding the 128-kDa *C. elegans* OGT protein (7). From existing EST data, this gene (*ogt-1*) appears to encode a single transcript corresponding to the nuclear/cytoplasmic form of OGT (7). Results obtained in our laboratory and others by using RNA interference (RNAi) suggested that interference with OGT expression resulted in no obvious developmental defect (7, 17, 18). These RNAi results suggested that it might be possible to study the signaling function of OGT without producing lethality.

In this report, we study an *ogt-1* deletion strain of *C. elegans* that exhibits no obvious developmental phenotype in homozygous animals. We demonstrate that nuclear pore complexes in the *ogt-1* mutant strain lack O-GlcNAc yet are capable of mediating the nuclear transport of transcription factors. Homozygous animals lacking *ogt-1* activity appear to develop normally with little change in growth rate or fertility. However, we do observe a striking increase in the levels of trehalose and glycogen and an accompanying decrease in fat stores in the *ogt-1* mutant strain. We also demonstrate that the *ogt-1* deletion allele genetically suppresses a constitutive dauer mutation, demonstrating that OGT modulates dauer formation in the nematode. These data suggest that in *C. elegans*, O-GlcNAc addition may play a regulatory, but nonessential, role in nematode development. The observed modulation of the dauer pathway by OGT-1 suggests that the nematode may be a genetically amenable model for studying nutrient-driven insulin resistance.

Materials and Methods

Strains. The following strains were used in this study: WT N2 Bristol, RB653 [*ogt-1(ok430)*] generated and kindly provided by the

This paper was submitted directly (Track II) to the PNAS office.

Abbreviations: O-GlcNAc, O-linked *N*-acetylglucosamine; OGT, O-GlcNAc transferase; RNAi, RNA interference.

†To whom correspondence should be addressed. E-mail: jah@helix.nih.gov.

C. elegans Gene Knockout Consortium (Oklahoma Medical Research Foundation, Oklahoma City), KM258 *ogt-1(ok430)* backcrossed four times, the integrated *skn-1*::*gfp* transgene (IS007) strain LD007 kindly provided by J. An and K. Blackwell (Joslin Diabetes Center, Boston), KM259 *ogt-1(ok430)*; IS007, *daf-2(e1370)*, *and ogt-1(ok430) daf-2(e1370)*.

Characterization of the *ogt-1(ok430)* Deletion Allele. After backcrossing, single *ogt-1(ok430)* adult animals were lysed and used as a template to amplify the *ogt-1* genomic region by using the original nested primers designed by the *C. elegans* Gene Knockout Consortium. The PCR products from several individual animal lysates were pooled and sequenced with primers spanning the region. Sequence analysis revealed that the *ogt-1(ok430)* allele resulted from a deletion of 1,094 bp of *ogt-1* gene sequence from the beginning of exon 8 to the middle of exon 9. In addition to the deleted sequence, this region had an insertion of 141 bp derived from noncoding sequence from cosmid F54E7 located ≈1,500 kb from *ogt-1* on LGIII. The inserted sequence results in an in-frame stop codon at the 5′ deletion breakpoint, resulting in a predicted truncated *ogt-1* translation product of 454 aa compared with the WT protein that is 1,151 aa in length. The deletion allele was subsequently tracked by nested PCR by using the outside pair of primers MWK453 (CCACACTTCCCTGATGCCTAC) and consortium "inner left" (ACCTGTCCGAGACCATTCTG) and the inside pair of primers MWK456 (CTCTGCCAACCCACGCGGA) and MWK457 (TGAGCGTGATCTCCAATGAAG). The predicted *ogt-1* mRNA in *ogt-1(ok430)* was confirmed by RT-PCR and sequencing.

Lipid Analysis. Lipids were extracted by the method of Folch *et al.* (19) after sonication of lyophilized nematode pellets in chloroform/methanol 2:1. After extraction, the lipids were subjected to two additional extractions in chloroform/methanol 2:1. Lipid fractions were then dried under nitrogen and analyzed by either TLC to separate lipid fractions [hexane/diethyl ether/acetic acid (70/30/1, vol/vol)] or quantitatively analyzed by HPLC. For HPLC, nonpolar lipids were separated basically as described (20). In brief, total lipids were dried under N_2, resuspended in hexane, and injected onto a Zorbax CN (Agilent Technologies, Palo Alto, CA) 150 × 4.6 mm (5 μm) column. Mobile phase A was hexane and mobile phase B was tert-butyl methyl ether, and the flow rate was 1 ml/min. Solvent B was set at 3% for 3 min, increased to 20% by 12 min and 100% by 17 min, and held at 100% for 5 min. The column was allowed to reequilibrate with 3% solvent B for 5 min before the next injection. Lipids were detected with a PL-ELS 2100 evaporative light scattering detector (Polymer Laboratories, Amherst, MA) with an evaporator temperature of 90°C, nebulizer temperature of 50°C, and a gas (N_2) flow rate of 2 liters per min. The peak containing triglycerides was identified by comparison to known standards (Sigma). Calibration for mass amounts was based on an external standard.

Carbohydrate Analysis. *C. elegans* strains grown in large quantities were rinsed with water to rid bacteria and then rocked in water at room temperature for 30 min to allow the gut to purge. Samples were pelleted, frozen on dry ice, and stored at −70°C until analyzed. Frozen *C. elegans* pellets were lyophilized before extraction. The resulting dry residue was not necessarily homogenous, and care was taken in removing aliquots for assay. In general, the entire pellet was dissolved in 1 M NaOH and centrifuged for 10 min at 10,000 rpm at 4°C. The supernatant was collected and the insoluble residue was reextracted at one-half volume. Both supernatants were pooled and stored frozen; the insoluble residue was rejected. For analysis of GlcNAcitol, alkaline β-elimination was performed and the product was analyzed by HPLC as described below. All, or aliquots, of the extract was passed over a P-2 column, 15 × 75 mm, (Bio-Rad) (21) and eluted in 0.02 M ammonium formate containing 0.02% NaN_3 at room temperature. Fractions of ≈1 ml were collected every 3 min. To determine the location of various components, individual fraction were assayed on a Dionex HPLC equipped with a pulsed amperometric detector (model PAD 2) and pellicular anion exchange column (PA 10, 4 × 250 mm). Trehalose and monomeric glucose were assayed directly as above in 18 mM NaOH; fractions containing polymeric glucose (which we will term glycogen) were hydrolyzed at 100°C for 4 h in 2 M trifluoroacetic acid before being assayed. The identified fractions were pooled, lyophilized, and taken up in 1 ml of water for final carbohydrate determination. The limit of detection for the monosaccharides is ≈10–40 nmol·mg dry weight.

Nile Red and Carminic Acid Staining. Carminic acid was introduced into the WT N2 Bristol and KM258 *ogt-1(ok430)* worms through feeding. Specifically, OP50 bacterial cells were inoculated into LB broth containing 1 mg/ml carminic acid and grown overnight at room temperature. This culture was then used to prepare bacterial lawns on standard nematode growth media agar plates (21). Worms were transferred to the carminic acid containing lawns as young adults, and their progeny were analyzed at larval stage 4 or young adult stages. Nile red staining of mixed-stage embryos and adults was carried out as described (22).

Immunoblotting. Nematodes were dissolved in 10 vol of boiling SDS sample buffer. SDS/PAGE and transfer were performed as described (16).

Immunofluorescence. Embryos were permeabilized by freeze cracking and fixed in paraformaldehyde and methanol as described (23). Whole larvae and adults were fixed as described by Finney and Ruvkun (24). Primary Abs for RL-1 (IgM) and RL-2 (IgG) (Affinity BioReagents, Neshanic Station, NJ) and CeMyoD (HLH-1) (IgG) were diluted 1:400 and incubated with fixed specimens overnight at 4°C. After washing, 1:400 dilutions of fluorescently conjugated secondary Abs (Jackson Immunological, West Grove, PA) were applied for 2 h at room temperature. Specimens were washed and stained with DAPI before mounting.

Results

The *ogt-1* deletion allele *(ok430)* was obtained from the *C. elegans* Knockout Consortium as a viable homozygote and was backcrossed four times before further study. The homozygous *ogt-1(ok430)* strain appeared phenotypically normal upon simple inspection. Sequencing the *ogt-1(ok430)* allele revealed a 1,094-bp deletion of *ogt-1* and a 141-bp insertion resulting in an in-frame stop codon at the deletion break point. Sequencing *ogt-1* cDNA products from WT and *ogt-1(ok430)* animals confirmed the predicted mRNA products. The predicted *C. elegans* OGT translation product in *ogt-1(ok430)* is a truncated 465-aa protein. The first 454 amino acids are from OGT-1, and 11 additional residues are added as a result of the genomic rearrangement before the first in-frame stop codon (Fig. 1*A*). It is unlikely that this altered transcript accumulates to significant levels because of nonsense-mediated decay that, in the worm, is regulated by the Smg system (25). Our previous studies suggest that, even if the aberrant message is translated, the truncated protein would not produce catalytically active enzyme (7), and we consider this allele to likely be a null. To directly measure O-GlcNAc levels, we monitored O-GlcNAcitol released after alkaline β-elimination (Fig. 1*B*). In N2, O-GlcNAcitol levels were ≈225 nmol/mg dry weight, whereas O-GlcNAcitol was undetectable (<40 nmol/mg dry weight) in *ogt-1(ok430)*. We also carried out an Affymetrix GeneChip analysis for mixed stage populations of *ogt-1(ok430)* and N2 to assess global changes in transcription. The results suggested that the variations between the gene expression pattern derived from replicate RNA preparations were larger than differences between the strains, consistent with the lack of obvious phenotype.

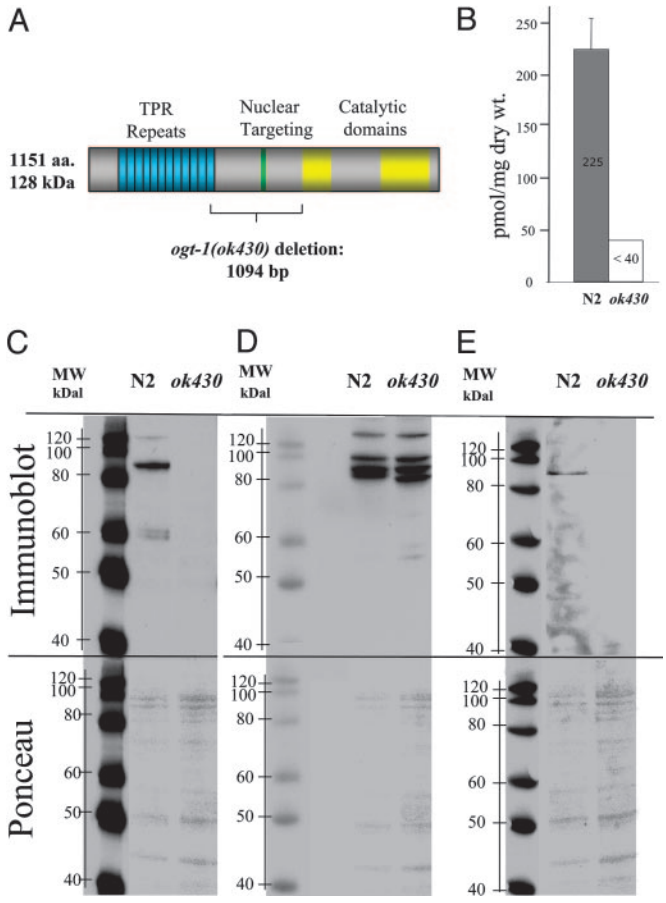

Fig. 1. A deletion in the *ogt-1* gene of *C. elegans* results in altered nuclear pore glycosylation. (*A*) Position of the deletion in *ogt-1(ok430)* is shown. The deletion removes the central portion of the protein producing a product lacking catalytic activity. (*B*) Levels of GlcNAcitol released by β elimination were measured. Nucleoporin-specific Abs directed against either O-GlcNAc (RL-2) (*C*) or protein determinants (RL-1) (*D*) were used to examine nuclear pore glycosylation in N2 and *ogt-1(ok430)* strains as indicated. (*E*) Another anti-O-GlcNAc Ab (CTD110) (27) was used for immunobloting. (*C–E Lower*) Corresponding Ponceau stains for each blot.

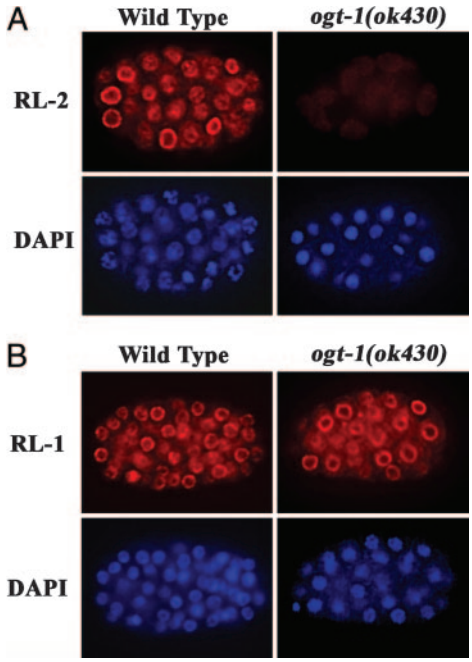

Fig. 2. O-GlcNAc is absent in *ogt-1(ok430)*. Embryos were fixed and processed as described in *Materials and Methods* and stained with either RL-2 (anti-O-GlcNAc) (*A*) or RL-1 (protein epitope) (*B*) mAbs to nucleoporins. DNA was stained with DAPI as indicated. No O-GlcNAc was detectable on nuclear pores in *ogt-1(ok430)* homozygous mutants.

To confirm that homozygous animals harboring the *ogt-1(ok430)* allele had lost the ability to transfer O-GlcNAc, we used two commercially available mAbs directed against nuclear pore antigens. The O-GlcNAc-specific Ab RL-2 recognizes O-GlcNAc-modified nucleoporins, whereas RL-1 recognizes nucleoporin protein determinants (26). Using immunoblotting, we analyzed the extracted proteins with both RL-1 and RL-2 in WT and *ogt-1(ok430)* mutant strains. Equal amounts of protein were loaded onto each gel lane (Fig. 1 *C–E*). As additional loading controls, blots were stained with Ponceau (Fig. 1 *C–E Lower*) before being analyzed by chemiluminescence (Fig. 1 *C–E Upper*). The anti-O-GlcNAc Ab RL-2 detected a number of apparently O-GlcNAc modified proteins in the WT extract ranging in molecular mass from ≈55 kDa to ≈150 kDa (Fig. 1*C*). These bands were not detected in *ogt-1(ok430)* protein extracts. As an internal loading control for the RL-2 experiments, we used RL-1, which binds to nucleoporin protein determinants. In contrast to the results with RL-2, nearly equivalent amounts of the nucleoporins were detected by using RL-1 in both strains (Fig. 1*D*). O-GlcNAc was also detected by using the O-GlcNAc Ab CTD110 (Fig. 1*E*) (27). Here again, bands were detectable in N2 but absent in *ogt-1(ok430)*.

We confirmed these biochemical findings by immunofluorescence microscopy. As shown in Fig. 2*A*, indirect immunofluorescence localization with RL-2 revealed a perinuclear distribution of nucleoporins in WT embryos that was absent in *ogt-1(ok430)* embryos. The position of the nucleus is apparent from the DAPI staining shown below for each embryo. In contrast, as shown in Fig. 2*B*, immunofluorescence with RL-1 demonstrated the normal amount and distribution of nucleoporins in both WT and *ogt-1(ok430)* embryos. These data suggest that the nucleoporins in *ogt-1(ok430)* are present but are not modified by O-GlcNAc.

Previous work has suggested that O-GlcNAc addition to nuclear pores may play a role in nuclear transport (1, 2). For example, the lectin wheat germ agglutinin interferes with nuclear transport by binding to O-GlcNAc residues on nuclear pore proteins. To examine the effect of altered O-GlcNAc synthesis on nuclear pore function, we examined nuclear transport of several well characterized *C. elegans* transcription factors, including SKN-1, HLH-1, HLH-2, ELT-2, and LIN-26. In *C. elegans*, SKN-1 is involved in both early blastomere development and the stress response (28–31). The stress response in larvae and adults causes cytoplasmic SKN-1 in intestinal cells to rapidly translocate to the nucleus (28). We have used the intestinal nuclear translocation of SKN-1 in response to sodium azide-induced stress to assay nuclear transport in *ogt-1(ok430)* animals. In Fig. 3*A*, SKN-1::GFP expression and localization was monitored in a WT and *ogt-1(ok430)* background. As shown in Fig. 3*A Left*, sodium azide induces the rapid appearance of SKN-1::GFP in intestinal cell nuclei. When the same experiment was carried out in the *ogt-1(ok430)* mutant background (Fig. 3*A Right*), a translocation with similar kinetics was observed. These data suggest that the OGT-deficient nuclear pores in *ogt-1(ok430)* are capable of mediating normal rates of nuclear import. We also examined another transcription factor, HLH-1, that appears early in development in the nucleus of muscle precursor cells undergoing rapid cell divisions (23, 32). Here again, the nuclear localization of the transcription factor in early development was indistinguishable in WT and *ogt-1(ok430)* strains (Fig. 3*B*). Similar results were obtained for HLH-2, ELT-2, and LIN-26 (data not shown). These findings suggest that nuclear transport of transcription factors in

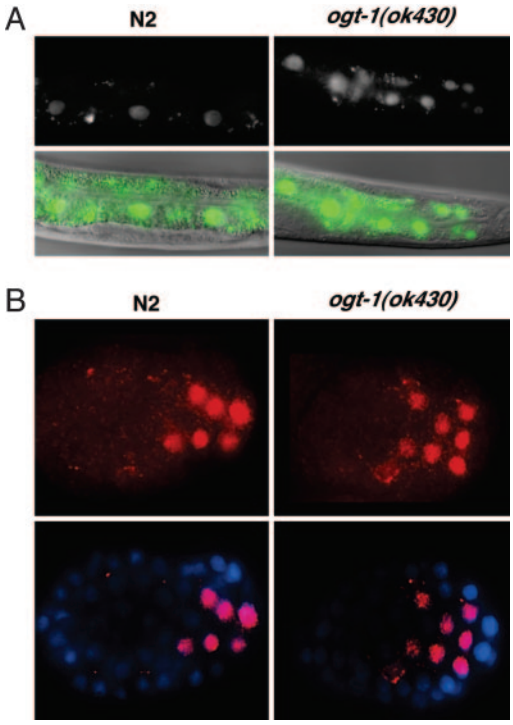

Fig. 3. Nuclear transport is unaffected in *ogt-1(ok430)*. The nuclear transport of transcription factors SKN-1 (*A*) and HLH-1 (*B*) was examined as described in *Materials and Methods*. (*A*) SKN-1 nuclear localization is shown (*Upper*) and overlaid onto a corresponding Nomarski image (*Lower*). (*B*) HLH-1 localization is shown (*Upper*) and overlaid upon a DAPI nuclear staining (*Lower*). Neither the kinetics of transport nor the nuclear localization of either transcription factor was noticeably altered in the *ogt-1(ok430)* mutant animals. Three other transcription factors, HLH-2, ELT-2, and LIN-26 showed similar results (data not shown).

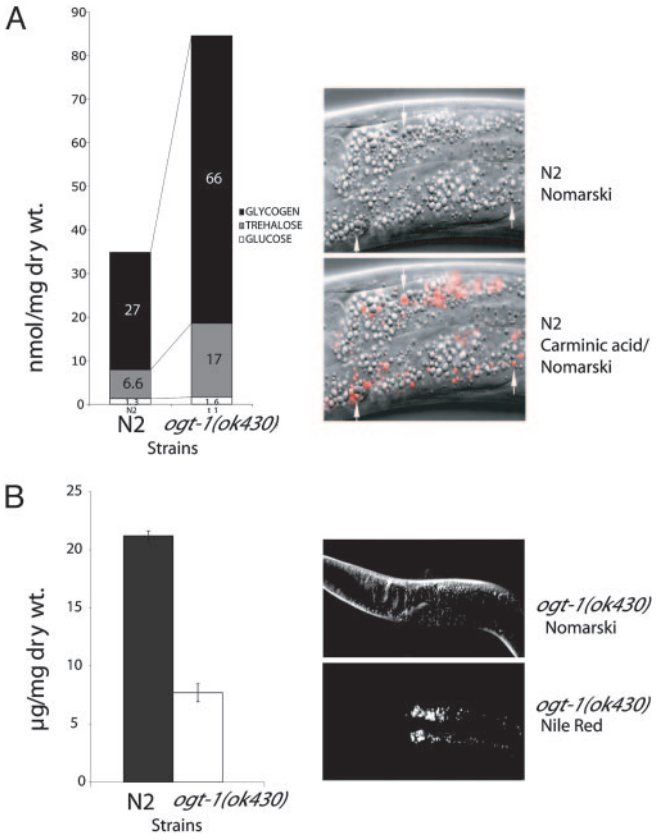

Fig. 4. Macronutrient storage in *ogt-1ok(430)*. N2 and *ogt-1(ok430)* strains were assayed for their storage of glycogen, trehalose, and glucose as described in *Materials and Methods*. (*A Left*) Levels of each of the stored carbohydrates is shown. A 2.5- to 3-fold elevation in sugar storage was observed; this representative experiment was repeated nine times with nearly identical results. (*A Right*) (*Lower*) Carminic acid was detected by fluorescence microscopy and was predominantly found in the intestine of the animal. The carminic acid-positive structures are a distinct subset of granules in the intestinal cells in both N2 and *ogt-1(ok430)*. (*Upper*) A corresponding Nomarski image is shown. (*B Left*) Storage of neutral lipids in N2 and *ogt-1(ok430)* was quantified in three replicate experiments as described in *Materials and Methods*. The reduction in neutral lipid storage was ≈70%. (*B Right*) (*Lower*) Enlargement of the anterior intestinal cells of the *ogt-1(ok430)* strain that was allowed to take up Nile red to label lipid droplets. (*Upper*) A corresponding Nomarski image is shown.

ogt-1(ok430) was unaffected. Although we cannot exclude the possibility that O-GlcNAc modification is required for nuclear targeting of some transcription factors, the normal development of *ogt-1(ok430)* suggests that O-GlcNAc modification is not an essential component of the nuclear transport machinery.

The hexosamine pathway terminating in OGT has been suggested to play a role in mammalian insulin resistance. Mammalian insulin resistance involves changes in carbohydrate and fat metabolism in insulin target tissues that become less responsive to circulating insulin levels. In *C. elegans*, an insulin-like-signaling pathway plays key roles in aging, development, dauer formation, and storage of macronutrients in granules (33–40). We sought to determine whether changes in carbohydrates or lipids occur as a result of the *ogt-1(ok430)* deletion. We measured the levels of monosaccharides, trehalose, and glycogen in mixed populations of both the WT (N2) and *ogt-1(ok430)* (Fig. 4*A Left*). The *ogt-1(ok430)* mutant strain showed a dramatic (2- to 3-fold) elevation of both trehalose and glycogen stores (Fig. 4*A*). The sugar storage phenotype was also observed after RNAi of the *ogt-1* locus in the N2 strain (1.6-fold). In contrast, RNAi of the *ogt-1* locus in the *ogt-1(ok430)* deletion strain did not further increase sugar storage as anticipated for an *ogt-1* null (both conditions ≈2.1-fold).

To determine the site of carbohydrate storage, we allowed *C. elegans* strains to take up carminic acid added to *Escherichia coli* as described in *Materials and Methods*. Carminic acid is a fluorescent derivative of glucose that binds to glycogen and trehalose (41, 42). As shown in Fig. 4*A Right*, stores of glycogen were readily visualized in the intestine by using carminic acid. Only a subset of the granules in intestinal cells were labeled, suggesting that glycogen storage is restricted to these structures in the gut. Other storage sites of glycogen storage may exist in *C. elegans* that were not labeled under these conditions.

To measure the storage of fat in the two strains, we performed a quantitative lipid analysis (see *Materials and Methods*). As shown in Fig. 4*B Left*, the results of several replicate experiments suggest that *ogt-1(ok430)* mutant animals stored only approximately one-third of the level of triglycerides observed in the N2 strain. Sterol esters were also reduced in *ogt-1(ok430)* mutant animals (data not shown). The site of accumulation of neutral lipids in both *ogt-1(ok430)* (Fig. 4*B Right*) and WT strains (data not shown) by using the fluorescent probe Nile red (5H-benzo-[a]-phenoxazine-5–1,9-diethylamino) was in a subset of granules in the intestine. These findings demonstrate a decrease in fat storage occurs in the absence of OGT activity. Decreased lipid storage is in contrast to the increase in carbohydrate stores observed in *ogt-1(ok430)* mutants (Fig. 4*A*).

The observed alteration in carbohydrate and lipid storage in *ogt-1(ok430)* suggested an alteration in insulin signaling. In nematodes, an insulin-like-signaling cascade is involved in macronutrient storage, longevity, and the transition to dauer (diapause) (Fig. 5*A*).

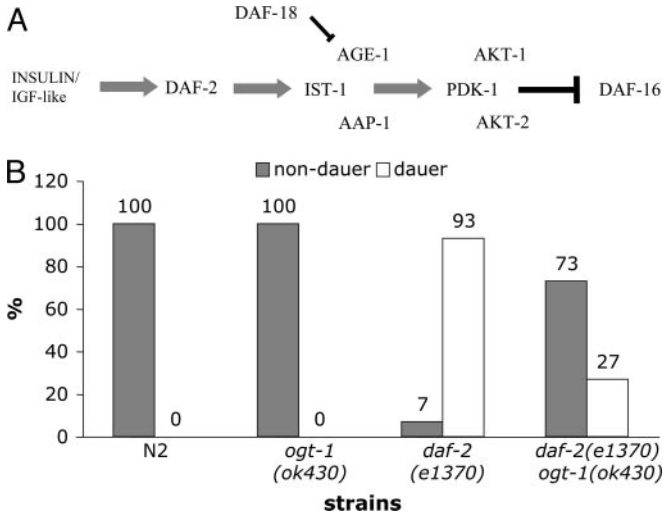

Fig. 5. Loss of OGT activity leads to alteration of dauer formation in *C. elegans*. (*A*) Insulin-like-signaling *C. elegans*. Key components of the insulin-like-signaling pathway leading to dauer formation are shown. Without DAF-2 signaling, DAF-16 is not repressed, and the dauer pathway is initiated. Mammalian homologs of the *C. elegans* proteins exist for each case. (*B*) Loss of OGT activity suppresses dauer formation. To test the role of *ogt-1* in the insulin-signaling pathway, we used an allele (*e1370)* of the *daf-2* gene that encodes an insulin-like receptor. At the restrictive temperature (25°C), *daf-2(e1370)* is a constitutive dauer with 100% of animals entering diapause. However, by culturing animals at slightly lower temperatures, the percentage of animals entering dauer can be manipulated. We tested temperatures at 0.5°C increments between 22°C and 24°C by incubating cultures in an Echotherm incubator (Torrey Pines Scientific, San Marcus, CA) with the temperature monitored by using a Barnant thermocouple thermometer (Barnant, Barrington, IL). We found that 22.5°C was the optimal temperature leading to sensitized *daf-2(e1370)* mutants for these assays. Adults of each strain tested were allowed to lay embryos overnight at 15°C. Cultures were shifted to 22.5°C and scored 3 d later. Animals scored as dauers were arrested and displayed canonical visible phenotypes; all other animals were scored as nondauers. At 22.5°C, no dauers were observed in cultures of N2 ($n = 222$) or *ogt-1(ok430)* mutants ($n = 432$), whereas *daf-2(e1370)* mutants had 93% dauers ($n = 579$). In contrast, *ogt-1(ok430) daf-2(e1370)* double mutant cultures had only 27% dauers ($n = 332$) at 22.5°C, demonstrating the loss of OGT-1 activity suppressed *daf-2(e1370)* dauer formation at this temperature.

Components of this pathway are conserved from nematodes to humans (33–40). To assess the impact of the *ogt-1(ok430)* null on insulin-like signaling, we crossed *ogt-1(ok 430)* to a strain harboring a temperature-sensitive constitutive mutation in *daf-2*, encoding an insulin-like receptor (67). As shown in Fig. 5*B*, we examined dauer development in N2, *ogt-1(ok430)*, *daf-2(e1370)*, and the *ogt-1(ok430) daf-2(e1370)* double mutant. Neither N2 nor *ogt-1(ok430)* produced dauers. In contrast, the *daf-2* mutant produced nearly 100% dauers under these conditions. In the *ogt-1(ok430) daf-2(e1370)* strain, the formation of dauers was greatly reduced, demonstrating that *ogt-1(ok430)* is a genetic suppressor of dauer formation induced by the *daf-2* ts allele. These data, coupled with the observed changes in macronutrient storage, implicate O-GlcNAc addition by OGT-1 in modulating insulin-like-signaling and/or parallel pathways regulating diapause in the nematode.

Discussion

OGT-1 Plays a Nonessential Regulatory Role in *C. elegans*. The isolation of a viable *C. elegans* strain lacking OGT activity allows a direct examination of the role of O-GlcNAc modification in the development and physiology of the nematode. Here we have demonstrated that nuclear pores in homozygous *ogt-1(ok430)* animals lacking O-GlcNAc are present in normal amounts and are capable of supporting normal nuclear transport of at least five transcription factors. We also observed no gross changes in the development of *ogt-1(ok430)* mutants. These findings are consistent with previous RNAi results from our own and other laboratories (7, 17, 18). Quite different results have been reported for OGT knockouts in mice where stem cell and embryonic lethality were observed (13, 14). The mice in the conditional knockout survive until embryonic day 8.5. The differences observed between the phenotypes in mammals and nematodes may be caused by the more complex nature of the mammalian gene. In *C. elegans*, we have reported the existence of a single gene, *ogt-1* (7). Unlike the *ogt-1*-related genes in *Arabidopsis* [*spindly* and *secret agent* (43)], there is no evidence for redundancy of *ogt-1* in the *C. elegans* genome (7). We have previously demonstrated the existence of multiple alternatively spliced transcripts in mouse and human that produce differentially targeted proteins (14). In *C. elegans*, the available ESTs suggest that only one isoform (corresponding to the nucleocytoplasmic OGT) is produced. Mammalian isoforms include 116-kDa nucleocytoplasmic OGT, the 78-kDa short OGT isoform, and the 103-kDa mitochondrially targeted isoform. The short OGT isoform has been implicated as an antiapoptotic gene in mammals (44). Another isoform is targeted to mitochondria and induces apoptosis when expressed in mammalian cells (D.C.L., S.H. Shin, and J.A.H., unpublished data). The pathway of apoptosis has been well characterized in *C. elegans* and involves a cascade of events resulting in caspase activation (45–47). The role of mitochondria in this process has been subject to much debate but may differ in detail from the mitochondrion's role in mammalian apoptosis (48–56). It is clear that absence of *ogt-1* in *C. elegans* does not lead to a dramatic alteration in programmed cell death.

OGT-1 Modulates Dauer Formation and Macronutrient Storage. In this report, we have shown that an *ogt-1* deletion allele suppresses dauer formation induced by the partial loss of function of *daf-2*, encoding an insulin-like receptor (Fig. 5). These data suggest that the hexosamine-signaling pathway terminating in OGT-1 may normally act to suppress insulin signaling in the nematode. In parallel findings, we have shown that the *ogt-1(ok430)* mutant strain, lacking OGT activity, has altered carbohydrate and lipid metabolism. Significantly higher levels of the circulating disaccharide trehalose and elevated glycogen stores are detected in *ogt-1(ok430)* mutants compared with WT animals. These findings are extremely interesting in light of the proposed function of OGT in nutrient-sensing pathways and the regulation of insulin signaling in mammals. Macronutrient storage occurs in the transition to dauer (diapause) in *C. elegans* in a process regulated by the insulin-like-signaling pathway (38). Furthermore, in mammals, the enzymes GSK-3β and glycogen synthase regulate glycogen stores downstream of insulin-signaling cascades (57–59). O-GlcNAc modification of glycogen synthase has been shown to inhibit the ability of the enzyme to catalyze glycogen formation. Several of the enzymes upstream of glycogen synthase, including GSK-3β, are also substrates for OGT (57–59). The sugar trehalose may be important in the physiology of nematodes where it functions in sugar transport, energy storage, and protection against environmental stress. Trehalose metabolism is catalyzed by trehalose-6-phosphate synthase and trehalose-6-phospate phosphatase, responsible for trehalose synthesis, and trehalase-catalyzing hydrolysis of the disaccharide. In *C. elegans*, the trehalase and trehalose-6-phosphate synthase genes are induced in *daf-2* mutants and repressed by *daf-16* (Forkhead transcription factor) RNAi (60). The *ogt-1(ok430)* mutant strain produces much higher levels of glycogen and trehalose than WT animals under normal culture conditions, suggesting that the absence of *ogt-1* leads to deregulation of these metabolic pathways. It is likely that O-GlcNAc addition normally plays a role in nutrient sensing by detecting flux through the hexosamine-synthetic pathway. This study provides genetic evidence that the nematode hexosamine-signaling pathway interacts with the insulin-signaling pathway, as previous data has suggested in mammals (1–4). The insulin-

signaling pathway is known to modulate lipid and carbohydrate storage in the nematode (38). With increased access to nutrients, a concomitant increase in O-GlcNAc modification would then serve to blunt insulin signaling. Based on what we know in mammals, the effects of the *ogt-1(ok430)* null in the nematode are also likely to include alteration of enzyme function, transcription, translation, and protein stability.

The decrease in neutral lipid storage in *ogt-1(ok430)* strongly suggests that alterations in cellular signaling accompany the knockout of OGT. Enzymes of lipid storage are transcriptionally responsive to the insulin-like-signaling pathways in *C. elegans* (22, 61–63), and elevated lipid storage occurs in dauer (64, 65). In humans, type 2 diabetes (noninsulin-dependent diabetes mellitus, adult onset) is characterized by elevated plasma fatty acids, which may result from unchecked lipolysis in adipose cells. In the nematode model provided by the *ogt-1(ok430)* mutant, it is not yet clear whether the lowered neutral lipid stores are caused by decreased synthesis of neutral lipids from nutrients or increased mobilization of triglycerides to form free fatty acids.

A Genetic Model of Insulin Resistance. The *C. elegans* strain lacking OGT-1 activity may provide a valuable tool for examining the role of O-GlcNAc addition in cellular function and human disease. For instance, the putative role of OGT in neurodegeneration may become accessible in the nematode. A nematode model of tauopathy and neurodegeneration has recently been described that will enable a dissection of the mechanism of neurodegeneration and the possible role of OGT in this process (66). We feel that the nematode may be a very useful model for examining the insulin resistance associated with noninsulin-dependent diabetes mellitus. OGT has been implicated in mammalian insulin resistance (1–4). We previously showed that OGT overexpression produces insulin resistance in transgenic mice (3). The present study suggests a modulation of dauer formation and macronutrient storage in the worm by OGT-1 that is analogous to metabolic changes associated with mammalian insulin resistance. In nematodes, dauer formation is influenced by insulin-signaling as well as parallel-signaling pathways (38). This genetic system offers clear advantages in sorting out the contribution of OGT and these other pathways to dauer formation. The interaction between the ''hexosamine-signaling pathway'' and the insulin-like signaling pathway may be amenable to genetic analysis.

We thank Othmar Gabriel for assistance with sugar nucleotide determination and carbohydrate analysis, Robert Littlejohn for technical help, and Drs. Eun Ju Kim and Brooke Lazarus for assistance with attempting to assay the nematode enzymes of O-GlcNAc addition.

1. Hanover, J. A. (2001) *FASEB J.* **15,** 1865–1876.
2. Wells, L., Vosseller, K. & Hart, G. W. (2001) *Science* **291,** 2376–2378.
3. McClain, D. A., Lubas, W. A., Cooksey, R. C., Hazel, M., Parker, G. J., Love, D. C. & Hanover, J. A. (2002) *Proc. Natl. Acad. Sci. USA* **99,** 10695–10699.
4. Vosseller, K., Wells, L., Lane, M. D. & Hart, G. W. (2002) *Proc. Natl. Acad. Sci. USA* **99,** 5313–5318.
5. Gao, Y., Wells, L., Comer, F. I., Parker, G. J. & Hart, G. W. (2001) *J. Biol. Chem.* **276,** 9838–9845.
6. Wells, L., Gao, Y., Mahoney, J. A., Vosseller, K., Chen, C., Rosen, A. & Hart, G. W. (2002) *J. Biol. Chem.* **277,** 1755–1761.
7. Lubas, W. A., Frank, D. W., Krause, M. & Hanover, J. A. (1997) *J. Biol. Chem.* **272,** 9316–9324.
8. Kreppel, L. K., Blomberg, M. A. & Hart, G. W. (1997) *J. Biol. Chem.* **272,** 9308–9315.
9. Swain, S. M., Tseng, T. S. & Olszewski, N. E. (2001) *Plant Physiol.* **126,** 1174–1185.
10. Thornton, T. M., Swain, S. M. & Olszewski, N. E. (1999) *Trends Plant Sci.* **4,** 424–428.
11. Jinek, M., Rehwinkel, J., Lazarus, B. D., Izaurralde, E., Hanover, J. A. & Conti, E. (2004) *Nat. Struct. Mol. Biol.* **11,** 1001–1007.
12. Wrabl, J. O. & Grishin, N. V. (2001) *J. Mol. Biol.* **314,** 365–374.
13. Shafi, R., Iyer, S. P., Ellies, L. G., O'Donnell, N., Marek, K. W., Chui, D., Hart, G. W. & Marth, J. D. (2000) *Proc. Natl. Acad. Sci. USA* **97,** 5735–5739.
14. Hanover, J. A., Yu, S., Lubas, W. B., Shin, S. H., Ragano-Caracciola, M., Kochran, J. & Love, D. C. (2003) *Arch. Biochem. Biophys.* **409,** 287–297.
15. O'Donnell, N., Zachara, N. E., Hart, G. W. & Marth, J. D. (2004) *Mol. Cell. Biol.* **24,** 1680–1690.
16. Love, D. C., Kochan, J., Cathey, R. L., Shin, S. H., Hanover, J. A. & Kochran, J. (2003) *J. Cell Sci.* **116,** 647–654.
17. Gonczy, P., Echeverri, C., Oegema, K., Coulson, A., Jones, S. J., Copley, R. R., Duperon, J., Oegema, J., Brehm, M., Cassin, E., *et al.* (2000) *Nature* **408,** 331–336.
18. Kamath, R. S., Fraser, A. G., Dong, Y., Poulin, G., Durbin, R., Gotta, M., Kanapin, A., Le, B. N., Moreno, S., Sohrmann, M., *et al.* (2003) *Nature* **421,** 231–237.
19. Folch, J., Sloane, S. G. H. & Lees, M. (1957) *J. Biol. Chem.* **226,** 497–509.
20. El Hamdy, A. H. (1993) *J. High Res. Chromatogr.* **16,** 55.
21. Brenner, S. (1974) *Genetics* **77,** 71–94.
22. Ashrafi, K., Chang, F. Y., Watts, J. L., Fraser, A. G., Kamath, R. S., Ahringer, J. & Ruvkun, G. (2003) *Nature* **421,** 268–272.
23. Krause, M., Fire, A., Harrison, S. W., Priess, J. & Weintraub, H. (1990) *Cell* **63,** 907–919.
24. Finney, M. & Ruvkun, G. (1990) *Cell* **63,** 895–905.
25. Pulak, R. & Anderson, P. (1993) *Genes Dev.* **7,** 1885–1897.
26. Snow, C. M., Senior, A. & Gerace, L. (1987) *J. Cell Biol.* **104,** 1143–1156.
27. Comer, F. I., Vosseller, K., Wells, L., Accavitti, M. A. & Hart, G. W. (2001) *Anal. Biochem.* **293,** 169–177.
28. An, J. H. & Blackwell, T. K. (2003) *Genes Dev.* **17,** 1882–1893.
29. Carroll, A. S., Gilbert, D. E., Liu, X., Cheung, J. W., Michnowicz, J. E., Wagner, G., Ellenberger, T. E. & Blackwell, T. K. (1997) *Genes Dev.* **11,** 2227–2238.
30. Walker, A. K., See, R., Batchelder, C., Kophengnavong, T., Gronniger, J. T., Shi, Y. & Blackwell, T. K. (2000) *J. Biol. Chem.* **275,** 22166–22171.
31. Bowerman, B., Eaton, B. A. & Priess, J. R. (1992) *Cell* **68,** 1061–1075.
32. Krause, M. (1995) *BioEssays* **17,** 219–228.
33. Cypser, J. R. & Johnson, T. E. (2003) *Biogerontology* **4,** 203–214.
34. Dorman, J. B., Albinder, B., Shroyer, T. & Kenyon, C. (1995) *Genetics* **141,** 1399–1406.
35. Gottlieb, S. & Ruvkun, G. (1994) *Genetics* **137,** 107–120.
36. Holt, S. J. & Riddle, D. L. (2003) *Mech. Ageing Dev.* **124,** 779–800.
37. Kenyon, C., Chang, J., Gensch, E., Rudner, A. & Tabtiang, R. (1993) *Nature* **366,** 461–464.
38. Kimura, K. D., Tissenbaum, H. A., Liu, Y. & Ruvkun, G. (1997) *Science* **277,** 942–946.
39. Rea, S. & Johnson, T. E. (2003) *Dev. Cell* **5,** 197–203.
40. Tissenbaum, H. A. & Ruvkun, G. (1998) *Genetics* **148,** 703–717.
41. Horobin, R. W. & Murgatroyd, L. B. (1971) *Histochem. J.* **3,** 1–9.
42. Rasimas, J. P., Berglund, K. A. & Blanchard, G. J. (1996) *J. Phys. Chem.* **100,** 7220–7229.
43. Hartweck, L. M., Scott, C. L. & Olszewski, N. E. (2002) *Genetics* **161,** 1279–1291.
44. Fletcher, B. S., Dragstedt, C., Notterpek, L. & Nolan, G. P. (2002) *Leukemia* **16,** 1507–1518.
45. Metzstein, M. M., Stanfield, G. M. & Horvitz, H. R. (1998) *Trends Genet.* **14,** 410–416.
46. Hengartner, M. O. (2001) *Cell* **104,** 325–328.
47. Kaufmann, S. H. & Hengartner, M. O. (2001) *Trends Cell Biol.* **11,** 526–534.
48. Adams, J. M. & Cory, S. (2002) *Curr. Opin. Cell Biol.* **14,** 715–720.
49. Adrain, C. & Martin, S. J. (2001) *Trends Biochem. Sci.* **26,** 390–397.
50. Parrish, J., Li, L., Klotz, K., Ledwich, D., Wang, X. & Xue, D. (2001) *Nature* **412,** 90–94.
51. Wang, X., Yang, C., Chai, J., Shi, Y. & Xue, D. (2002) *Science* **298,** 1587–1592.
52. Borner, C. & Monney, L. (1999) *Cell Death Differ.* **6,** 497–507.
53. Mignotte, B. & Vayssiere, J. L. (1998) *Eur. J. Biochem.* **252,** 1–15.
54. Gottlieb, R. A. (2000) *FEBS Lett.* **482,** 6–12.
55. Bloss, T. A., Witze, E. S. & Rothman, J. H. (2003) *Nature* **424,** 1066–1071.
56. Lee, S. S., Lee, R. Y., Fraser, A. G., Kamath, R. S., Ahringer, J. & Ruvkun, G. (2003) *Nat. Genet.* **33,** 40–48.
57. Parker, G., Taylor, R., Jones, D. & McClain, D. (2004) *J. Biol. Chem.* **279,** 20636–20642.
58. Parker, G. J., Lund, K. C., Taylor, R. P. & McClain, D. A. (2003) *J. Biol. Chem.* **278,** 10022–10027.
59. Lubas, W. A. & Hanover, J. A. (2000) *J. Biol. Chem.* **275,** 10983–10988.
60. Murphy, C. T., McCarroll, S. A., Bargmann, C. I., Fraser, A., Kamath, R. S., Ahringer, J., Li, H. & Kenyon, C. (2003) *Nature* **424,** 277–283.
61. Ambros, V. (2003) *Cell* **113,** 673–676.
62. Baehrecke, E. H. (2002) *Nat. Rev. Mol. Cell. Biol.* **3,** 779–787.
63. Chiang, S. H. & MacDougald, O. A. (2003) *Trends Genet.* **19,** 523–525.
64. Ogg, S., Paradis, S., Gottlieb, S., Patterson, G. I., Lee, L., Tissenbaum, H. A. & Ruvkun, G. (1997) *Nature* **389,** 994–999.
65. Sze, J. Y., Victor, M., Loer, C., Shi, Y. & Ruvkun, G. (2000) *Nature* **403,** 560–564.
66. Kraemer, B. C., Zhang, B., Leverenz, J. B., Thomas, J. H., Trojanowski, J. Q. & Schellenberg, G. D. (2003) *Proc. Natl. Acad. Sci. USA* **100,** 9980–9985.
67. Riddle, D. L. (1977) *Stadler Genet. Symp. Ser.* **9,** 101–120.